Fuel 241 (2019) 725–732

Contents lists available at ScienceDirect

Fuel

journal homepage: www.elsevier.com/locate/fuel

Full Length Article

Hansen solubility parameters and thermodynamic modeling for LLE description during glycerol-settling in ester production from coconut oil

Otto Alberto Quispe Jimenez[a], Vanessa Vilela Lemos[a], Eduardo Augusto Caldas Batista[b], Marlus Pinheiro Rolemberg[a], Rodrigo Corrêa Basso[a,*]

[a] Institute of Science and Technology, Federal University of Alfenas (Unifal-MG), 37715-400 Poços de Caldas, Minas Gerais, Brazil
[b] Laboratory of Extraction, Applied Thermodynamics and Equilibrium (ExTrAE), School of Food Engineering, Department of Food Engineering, University of Campinas (UNICAMP), 13083-862 Campinas, São Paulo, Brazil

GRAPHICAL ABSTRACT

Esters: (■) $C_{10}H_{20}O_2$; (▲) $C_{12}H_{24}O_2$; (●) $C_{14}H_{28}O_2$; (□) $C_{16}H_{32}O_2$; (Δ) $C_{18}H_{36}O_2$; (♦) $C_{20}H_{40}O_2$; (◇) $C_{20}H_{38}O_2$; (○)$C_{20}H_{36}O_2$. (◄) glycerol. (►) ethanol. (×) glycerol-rich phase. (+) ester-rich phase.

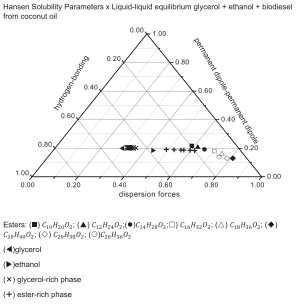

ARTICLE INFO

Keywords:
Hansen solubility parameters
Liquid–liquid equilibrium
Ethyl ester
Glycerol-settling step
Thermodynamic modeling
Ester partition

ABSTRACT

The liquid–liquid equilibrium behavior is important when describing the separation of components involved in alkyl ester production during the glycerol-settling step. Therefore, this study presents original data on a liquid–liquid equilibrium system composed of glycerol + ethanol + ethyl esters from coconut oil at 298 K using an untapped approach based on the Hansen solubility parameters describing the individual ethyl ester distribution between the glycerol and ester rich phases. The difference in average molar masses of the ester mixtures in both phases when compared to fatty acid alkyl ester in overall composition reaches more than 10% depending on the ethanol content in the overall composition. The individual partition of ethyl esters in the glycerol-rich phase increases as result of the decrease in molecular size of this class of components. This behavior was shown based on the smaller difference in Hansen solubility parameters among esters with less carbon and the glycerol-rich phases as compared to esters with longer carbon chain atoms. Deviations between the experimental and calculated mass fractions were 0.83%, 4.07%, and 0.87% when using NRTL, UNIFAC-LLE, and UNIFAC-OHgly.

* Corresponding author.
E-mail address: rodrigo.c.basso@gmail.com (R.C. Basso).

https://doi.org/10.1016/j.fuel.2018.12.029
Received 22 August 2018; Received in revised form 5 December 2018; Accepted 7 December 2018

1. Introduction

Esters from fatty compounds have diverse technological uses. Fatty alcohols are produced for use as intermediates in the chemical industry for products including surfactants or cleaning supplies. The use of branched fatty acid alkyl esters as lubricants is attractive from an environmental perspective owing to their improved biodegradability. Such compounds have similar or better solvent properties as compared to hydrocarbons. The use of certain esters from vegetable oils as plasticizers have been proposed in the polymer industry, and long-chain alkyl esters can be used as high boiling point absorbents of nonpolar gases for the scrubbing of industrial emissions [1–5]. Additionally, alkyl ester mixtures obtained from fatty materials have been used as alternatives to diesel fuel. Some advantages of this biofuel as compared to diesel are its renewability, non-toxicity, availability, absence of sulfur and aromatic compounds, high cetane number, improved lubricating qualities, higher combustion efficiency, simple and short production time, and available production in most countries utilizing different raw materials [6–8].

The use of ethanol for fatty acid alkyl ester production as compared to methanol presents certain drawbacks that need solving to make this process technically and economically feasible. However, the use of ethanol is advantageous from ecological and safety perspectives because, in contrast to methanol, which is mainly produced from fossil fuels, ethanol is produced from the fermentation of several different crops, resulting in a complete bio-renewable and agricultural product. In addition, methanol is highly toxic compared to ethanol [9,10]. One of the main routes for the synthesis of alkyl esters is the transesterification of glyceride species with alcohol. Depending on the synthesis process, which may include enzymatic, alkaline catalysis, and acid catalysis using supercritical alcohol, the molar alcohol-to-oil ratio varies from 6:1 to 50:1 [11–13]. The ethanol concentration in the mixture determines the phase separation behavior in the first step of biodiesel production, during which glycerol is separated from biodiesel through a settling process, resulting in a glycerol-rich phase (GRP) and an ester-rich phase (ERP). As result of this behavior, research into the liquid–liquid equilibrium (LLE) in systems containing a fatty acid ethyl ester mixture + ethanol + glycerol is extremely important for an understanding, prediction, and design of this particular process.

A large number of chemical components in equilibrium systems complicate the thermodynamic modeling because a great number of binary interaction parameters are required to describe the equilibrium behavior. Consequently, a large amount of experimental data is needed for the model fitting owing to the large number of degrees of freedom. A pseudocomponent approach is used when an equilibrium system is made up of compounds having similar thermodynamic properties. During this procedure, these components are separated into pseudocomponents representing the real mixture properties that affect the equilibrium. The classic pseudocomponent procedure based on the vapor–liquid equilibrium properties cannot be used in LLE because this equilibrium is strongly affected by the chemical structure of the molecules. However, the average molar mass calculated from an individual component mixture having a similar chemical structure has been used in the pseudocomponent approach for LLE modeling [14–16].

The partition of nonelectrolytes between two liquid phases cannot be successful described based on macroscopic properties such as the dielectric constant or dipole moment. The application of Hildebrand's solubility parameters is a reasonable method for describing this behavior, showing a good correlation with the partition coefficient in a liquid system [17]. Because Hildebrand's method does not take into account the association among molecules based on the polar or hydrogen-bonding interactions, the solubility parameter approach was proposed by Hansen as an alternative method for evaluating the interactions among molecules. This last theory considers the effects of atomic dispersion forces, molecular permanent dipole-permanent dipole forces, and molecular hydrogen-bonding, as represented by the parameters δ_d, δ_p, and δ_{hb}, respectively [18–20].

A large number of studies have addressed LLE data for systems containing glycerol + short chain alcohol + ethyl ester mixture treated as a pseudocomponent, but only three [21–23] have studied the individual partition of alkyl esters in a complex mixture of this chemical class of components. In addition, no studies have reported and/or explained the differentiation in ester partition as result of the carbon chain length and number of saturations of molecules between the GRP and ERP in systems related to the glycerol-settling step during ester production. Therefore, the objectives of this study were to determine experimental LLE data of a system containing glycerol (1) + ethanol (2) + fatty acid ethyl esters (3) from coconut oil at 298 K, and explaining the partition of individual ethyl esters between GRP and ERP using an unusual approach based on the Hansen solubility parameters (HSPs). In addition, thermodynamic models were used to describe the LLE of the system using a pseudocomponent approach for the NRTL model, as well as an individual component approach based on UNIFAC-LLE and UNIFAC-OHgly [24].

2. Experimental procedure

2.1. Materials

Refined coconut oil was used for ethyl biodiesel production.

Glycerol (Sigma, > 0.99), ethanol (Merk, > 0.999), methanol (Honeywell, 0.9999) and anhydrous sodium hydroxide (Carlo Erba, > 0.97) were used in several steps of this study.

2.2. Production of distilled biodiesel from coconut oil

Aiming the removal of impurities such as soap, glycerol, ethanol, catalyst, monoacylglycerols and diacylglycerols, and other byproducts, the ethyl ester mixture from coconut oil was synthesized, washed, and distilled following the procedure described in the literature [21].

The ethyl ester mixture profile of the mixture obtained is shown in Table 1.

2.3. LLE experiments

Components were weighted on an analytical balance (Adam Equipment, model AAA160L ± 0.0001 g). Experimental LLE data were determined using headspace tubes (20 mL) vigorously stirred on a vortex (Phoenix, model AP56) and then centrifuged (Centrifuge Jouan, model BR4i) for 300 s at 4000 rpm. All systems were left at rest for at least 12 h at 298 K in a controlled thermostatic bath (Paar Physica, model VT2 $T \pm 0.2$ K). The system was considered to be in equilibrium when a defined interface and two clear layers were formed in the tubes, with the top and bottom layers constituting the ERP and GRP, respectively.

The expression "fatty acid alkyl esters" FAEE was used to designate, the mixtures of alkyl esters in the overall composition and the mixtures

Table 1
Experimental composition of FAEE from coconut oil in mass percentage.

Ester name	Molecular formula	MM ($g mol^{-1}$)	$100w$[a]
Octanoic acid ethyl ester	$C_{10}H_{20}O_2$	172.26	2.92
Decanoic acid ethyl ester	$C_{12}H_{24}O_2$	200.32	3.12
Dodecanoic acid ethyl ester	$C_{14}H_{28}O_2$	228.37	48.57
Tetradecanoic acid ethyl ester	$C_{16}H_{32}O_2$	256.42	16.80
Hexadecanoic acid ethyl ester	$C_{18}H_{36}O_2$	284.48	8.90
Ethyl octadecanoate	$C_{20}H_{40}O_2$	312.53	2.10
9-Octadecenoic acid ethyl ester	$C_{20}H_{38}O_2$	310.51	15.65
9,12-Octadecadienoic acid Ethyl ester	$C_{20}H_{36}O_2$	308.50	1.94

[a] Mass fraction of the ethyl ester.

of alkyl esters in the equilibrium phases.

2.4. Analytical methodology

The composition of FAEE in overall composition (Table 1) was determined in triplicate using a Perkin Elmer Clarus 600 gas chromatographic system, FID detector, and Elite capillary column (crossbond, 50% cyanopropylmethyl and 50% phenylmethyl polysiloxane) measuring 30 m in length, 0.25 mm internal diameter, and 0.25 μm in film thickness according to the methodology describe in the literature [21].

Quantitations of glycerol, ethanol and individual esters in each equilibrium phase were determined in at least triplicate using an Agilent capillary column (crossbond, 50% dimethylplolysiloxane and 50% cyanopropyl-phenil) with dimensions of 0.25 μm, 0.25 mm, and 30 m for the film thickness, internal diameter, and length, respectively, in the equipment described above, as well as a method previously developed specifically for this analysis under the following conditions: an injector and detector temperature of 523 K; an oven temperature of 313 K for 1 min, between 313 and 333 K at temperature rate of 5 K/min and held at 333 K for 1 min, between 333 K and 473 K at a temperature rate of 25 K/min and held at 473 K for 1 min, between 473 K and 508 K at a temperature rate of 7 K/min and held at 508 K for 1 min; a helium carrier gas of 1 mL/min for 5 min, 2.5 mL/min for 6 min, and 1.5 mL until the end of the experiment; a 1:40 split; and an injected volume of 0.4 μL [21].

The components were quantified based on an external calibration.

3. Theoretical calculations

3.1. Calculations of deviation in mass balance of the phases

The validity of the equilibrium experiments was confirmed according to a procedure reported by Marcilla [25] and calculated using spreadsheets developed by Rodrigues [26]. This method is based on a comparison of the sum of the calculated mass in both liquid phases with the actual total mass value used in the initial mixture, and therefore a relative deviation for each point of the overall mixture was obtained.

This approach uses independent component balances, totalizing K balances, given by Eq. (1):

$$M^{OC}w_i^{OC} = M^{GRP}w_i^{GRP} + M^{ERP}w_i^{ERP} \quad (1)$$

where i describes each individual component; M^{OC} is the mass of the overall composition; M^{GRP} and M^{ERP} are the total masses of the GRP and ERP, respectively; w_i^{OC} is the mass fraction of component i in the initial mixture; and w_i^{GRP} w_i^{ERP} are the mass fractions of component i in GRP and ERP, respectively.

After the calculations using equations representing the K balances, the values of M^{GRP} and M^{ERP} were obtained. The sum of M^{GRP} and M^{ERP} was compared to M^{OC} to calculate the deviations in overall mass balance using Eq. (2):

$$\delta(\%) = 100\cdot|(M^{GRP} + M^{ERP}) - M^{OC}|/M^{OC} \quad (2)$$

The relative average deviation in the mass balance of each component is calculated using Eq. (3):

$$\delta_i(\%) = \sum_n^N \left(100\cdot\frac{|(w_{i,n}^{GRP}M^{GRP} - w_{i,n}^{ERP}M^{ERP}) - w_{i,n}^{OC}M^{OC}|}{w_{i,n}^{OC}M^{OC}}\right)/N \quad (3)$$

where n is the tie line number and N is the total number of tie lines.

3.2. Distribution of ethyl esters between GRP and ERP

The deviations in the average molar mass of FAEE in the GRP and ERP from the average molar mass of FAEE in the overall composition were calculated using Eq. (4).

$$dMM = 100\cdot|\bar{M}^p - \bar{M}^{oc}|/\bar{M}^{oc} \quad (4)$$

where $\bar{M}^p$ is the average molar mass of FAEE in the GRP or ERP, and $\bar{M}^{oc}$ is the average molar mass of the FAEE mixture obtained from the transesterification reaction in the overall composition.

The partition coefficient was calculated using Eq. (5).

$$k = w_{ester}^{GP}/w_{ester}^{EP} \quad (5)$$

3.3. NRTL thermodynamic modeling

Experimental LLE data for the system were used to adjust the binary interaction parameters of the NRTL model. Despite the differences in distribution of the individual ethyl esters between phases in the LLE, the pseudocomponent approach was used to represent this component class. Thus, the FAEE was treated as an individual ethyl ester having the average molar mass of biodiesel. Therefore, the adjustments were conducted by considering the systems as pseudoternary for NRTL modeling. Because the FAEE contains eight individual esters, this mathematical approach is necessary to reduce the number of experimental data points required to adjust the NRTL binary interaction parameters. Otherwise, the modeling of the LLE behavior considering the ten individual components of the system would require the adjustment of 135 binary interaction parameters.

The mass fractions were used to report the composition owing to the difference in molar masses of the components. From this approach, the activity coefficient for the LLE is expressed through Eq. (6).

$$\gamma_i^w = \gamma_i/\left(M_i\sum_j^K \frac{w_j}{M_j}\right) \quad (6)$$

where $\gamma_i$is the activity coefficient calculated according to the NRTL model; γ_i^w is the activity coefficient expressed on a mass fraction basis; and w_i and M_i are the mass fraction and molar mass of the components, respectively; and i represents the component number.

The procedure used for estimating the NRTL parameters involves flash calculations for the midpoint composition of the experimental tie lines, and is based on the algorithm developed by Stragevitch and d'Avila [27], consisting of minimizing the objective function of the composition according to Eq. (7):

$$OF_w = \sum_m^D\sum_n^N\sum_i^{K-1}\left[\left(\frac{w_{i,n,m}^{GRP,expt} - w_{i,n,m}^{GRP,calc}}{\sigma_{w_{i,n,m}^{GRP}}}\right)^2 + \left(\frac{w_{i,n,m}^{ERP,expt} - w_{i,n,m}^{ERP,calc}}{\sigma_{w_{i,n,m}^{ERP}}}\right)^2\right] \quad (7)$$

where D is the is the number of data groups; N is the number of tie lines; K is the number of components; w is the mass fraction of the components; subscripts i, n, and m represent the component, tie line, and group number, respectively; exp and calc denote experimental data and calculated values; GRP and ERP denote the glycerol-rich and ester-rich phases, respectively; and σ is the standard deviation obtained for the composition of each phase.

The average relative deviations between the calculated mass fractions and experimental data were determined using Eq. (8).

$$w(\%) = \left\{\frac{\sum_n^N\sum_i^K[(W_{i,n}^{GRP,exp} - W_{i,n}^{GRP,calc})^2 + (W_{i,n}^{ERP,exp} - W_{i,n}^{ERP,calc})^2]}{2NK}\right\}^{1/2} \quad (8)$$

3.4. UNIFAC-LLE and UNIFAC-OHgly

The UNIFAC thermodynamic model was used to predict the LLE of the experimental data. Two parameter sets were evaluated to test the prediction capability of the model. The first, UNIFAC-LLE, with the structural molecular groups CH_3, CH_2, CH, CH=CH, CH_2COO, and OH, was reported by Fredenslund et al. [28], and their binary interaction parameter values for predicting the LLE behavior were updated by

Table 2
Experimental LLE data for the system glycerol (1) + ethanol (2) + FAEE (3) at 298 K, using the pseudoternary approach.

TL[a]	Overall Composition			Glycerol Rich Phase			Ester Rich Phase			δ(%)[b]
	w_1	w_2	w_3	w_1	w_2	w_3	w_1	w_2	w_3	
1	0.2021	0.397	0.4009	0.3904	0.5156	0.094	0.0707	0.3387	0.5906	0.50
2	0.2451	0.355	0.3999	0.4819	0.4717	0.0465	0.0438	0.2705	0.6857	0.15
3	0.2932	0.2959	0.4109	0.5711	0.409	0.0199	0.0264	0.2127	0.7609	0.04
4	0.3425	0.2640	0.3934	0.6503	0.3384	0.0113	0.0197	0.1892	0.7911	0.03
5	0.3899	0.2072	0.4030	0.7115	0.2836	0.0049	0.0134	0.1367	0.8499	0.40
6	0.4409	0.1598	0.3993	0.7774	0.2208	0.0018	0.0070	0.1033	0.8897	0.60

[a] Tie line identification number.
[b] Overall mass balance deviation calculated by Eq. (2).

Magnussen et al. [29]. The second, UNIFAL-OHgly, containing the same set of molecular groups with readjusted parameter values, in addition to a new molecular group, OHgly, was created to represent the OH group attached to the glycerol molecule, as reported by Bessa et al. [24].

UNIFAC modeling was conducted using all eight individual ethyl esters, considering a system composed of eight esters + glycerol + ethanol. Solely for the representation of the LLE, the ethyl ester mixture was grouped into a single pseudocomponent.

3.5. Hansen solubility parameters

The HSPs for each ethyl ester were calculated using only Eqs. (9)–(11), from the group contribution method proposed by Stefanis and Panayiotou, and updated by Stefanis and Panayiotou [30,31].

$$\delta_d = \left(\sum_i N_i C_i + \sum_i M_j D_j + 959.11 \right)^{0.4126} \tag{9}$$

$$\delta_p = \left(\sum_i N_i C_i + \sum_i M_j D_j + 7.6134 \right) \tag{10}$$

$$\delta_{hb} = \left(\sum_i N_i C_i + \sum_i M_j D_j + 2.6560 \right) \tag{11}$$

where $\delta_d (MPa^{1/2})$ is the dispersion solubility parameter, $\delta_p (MPa^{1/2})$ is the polar solubility parameter, $\delta_{hb} (MPa^{1/2})$ is the hydrogen bonding solubility parameter, C_i is the contribution of the first-order group i that appears N_i times in the molecule, and D_j is the contribution of the second-order group j that appears M_j times.

The total solubility parameter, $\delta_t (MPa^{1/2})$, for each component obtained from the interactions of the atomic dispersion forces, molecular permanent dipole–permanent dipole forces, and molecular hydrogen bonding is calculated using Eq. (12) [18,19].

$$\delta_t = (\delta_d^2 + \delta_p^2 + \delta_{hb}^2)^{1/2} \tag{12}$$

The three HSPs for the component mixtures in the GRP and ERP were calculated from the volume fraction using Eq. (13) [20].

$$\delta = \sum_i \varphi_i \delta_i \tag{13}$$

where

$$\varphi_i = (w_i/\rho_i) / \sum_i (w_i/\rho_i) \tag{14}$$

Here, δ $(MPa^{1/2})$ are the HSPs (δ_d, δ_p, or δ_{hb}) for the mixture of components i, φ is the volume fraction calculated using Eq. (14), and ρ is the component density calculated from the molar volume obtained through the group contribution model reported by Constantinou et al. [32].

HSPs were plotted using the diagram proposed by Teas, where each parameter (δ_d, δ_p, δ_{hb}) is represented by a single point on a ternary graph, calculated through the following Eqs. (15)–(17) [33]:

$$100 f_d = 100\delta_d / (\delta_d + \delta_p + \delta_{hb}) \tag{15}$$

$$100 f_p = 100\delta_p / (\delta_d + \delta_p + \delta_{hb}) \tag{16}$$

$$100 f_{hb} = 100\delta_{hb} / (\delta_d + \delta_p + \delta_{hb}) \tag{17}$$

4. Results and discussion

FAEE from coconut oil contains ethyl laurate and ethyl myristate, which are saturated esters composed of 14 and 16 carbon atoms, respectively, as the major components, totaling more than 65% of the entire mixture. Ethyl oleate, an unsaturated ester presenting 20 carbon atoms, is the third-most representative component, representing 15.7% of the total ester mixture. The high content of saturated ethyl esters containing up to 16 carbon atoms and monounsaturated ester improve the FAEE oxidative stability while not resulting in a higher melting point. This composition is favorable for the production of esters used as surfactants in the chemical and cosmetic industries, high performance lubricants, solvents for flavorings, plasticizers, and other start materials in the oleochemical industry. In some countries, mainly in southeast Asia, esters from coconut oil with a high acid content have been considered a possible raw material for biodiesel production once the high free fatty acid composition makes this oil a relatively low-cost raw material [34–36].

The average molar mass of FAEE in overall composition equal to 246.66 g·mol^{-1} was calculated from the eight ethyl esters quantified using gas chromatography (Table 1). This value was used as a reference to evaluate the deviations in the average molar mass of FAEE in the GRP and ERP.

The mass fraction compositions of the overall experimental data, and the correspondent tie lines for the system glycerol (1) + ethanol (2) + FAEE (3) using the pseudoternary approach, are presented in Table 2. The overall deviations in the mass balance per tie line (Eq. (2)) equal to or lower than 0.60% indicate the high quality of the experimental data. The average deviations per component (Eq. (3)) were 1.25%, 2.97%, and 0.44%, respectively, for glycerol, ethanol, and FAEE.

Fig. 1 shows ethanol distribution in the GRP and ERP, with high affinity for the former, as shown by the tie line slopes. A similar behavior was observed in the system containing glycerol + methanol + methyl oleate when methanol showed a higher partition to a glycerol-rich phase than to an ester-rich phase [37]. On the other hand, FAEE and glycerol are only slightly miscible, and their distribution between the phases is determined based on the ethanol mass fraction in the overall composition because high concentrations of this alcohol cause a higher miscibility between the components. This behavior indicates that a decrease in the ethanol mass fraction before the glycerol-settling step, and after the transesterification reaction ends, can reduce the biodiesel losses to the GRP, improving the glycerol purity during biodiesel production.

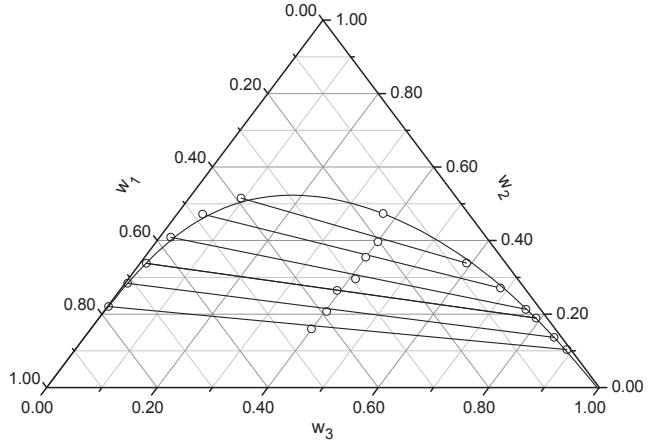

Fig. 1. LLE for the pseudoternary system glycerol (1) + ethanol (2) + FAEE (3) at 298 K: (w) mass fraction of the component or pseudocomponent; (○) experimental data; (—) NRTL calculated values.

The biphasic region for the system containing glycerol + ethanol + FAEE from coconut oil is smaller than the biphasic region observed for systems containing glycerol + methanol + commercial biodiesel (majority esters, 36.8% methyl oleate, 33.0% methyl linoleate, and 14.7% methyl palmitate) and glycerol + methanol + methyl biodiesel from soybean or palm oil [38,39]. This behavior results in a higher miscibility of esters with a small carbon chain, such as those from coconut oil, in the glycerol-rich phase, and a lower ethanol affinity for a glycerol-rich phase as compared to methanol.

The similarity between the experimental data and the calculated mass fractions using the NRTL model shows a good fit of the parameters, as presented in Table 3. The average relative deviation between the experimental data and calculated mass fractions is low (0.83%). Regardless of a different partition of the individual ethyl esters between the GRP and ERP, the use of the pseudocomponent approach did not reduce the applicability of the model when the focus is the distribution of biodiesel as a single compound, showing the descriptive power of the LLE behavior for the entire system. Using the pseudocomponent approach for NRTL and UNIQUAC modeling, other authors have reported the proper description of LLE behavior in commonly studied systems to represent the glycerol settling step [40,41] and washing step [42] in the biodiesel production process.

The UNIFAC-LLE model overestimates and underestimates the ethanol mass fractions in the GRP and ERP, respectively, when grouping all individual ethyl esters to represent the LLE behavior of this system, as shown in Fig. 2. UNIFAC-OHgly presented an improved description for such equilibrium behavior. The average deviations between the experimental data and calculated values (Eq. (8)) using UNIFAC-LLE and UNIFAC-OHgly were 4.07% and 0.87%, respectively, showing an improved prediction capability of the model owing to a parameter readjustment and the creation of the OHgly group. In contrast, the capability of the UNIFAC-OHgly to represent the individual ethyl ester mass fractions is poor, as shown in Table 4. The new UNIFAC-OHgly approach cannot properly represent the mass fractions of the individual ethyl esters in the GRP, mainly for saturated ethyl esters presenting less than eighteen carbon atoms per molecule, resulting in higher average deviations when compared to the experimental values than in the UNIFAC-LLE model.

Table 3
NRTL binary interaction parameters for the system glycerol (1) + ethanol (2) + FAEE (3).

Pair (ij)	A (0) ij	A (0) ji	α(0) ij = α (0) ji
12	−2640.200	429.800	0.5687
13	4302.700	349.300	0.1000
23	312.820	2656.200	0.5064

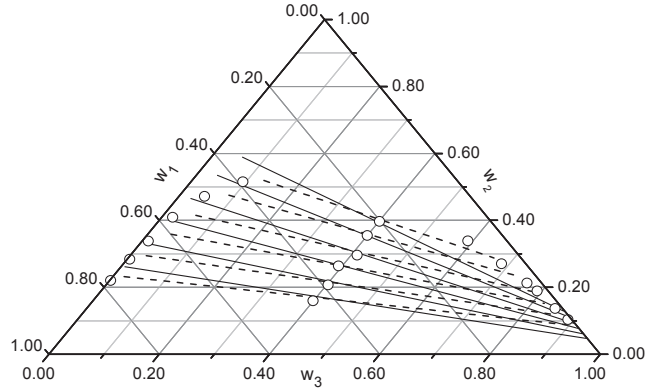

Fig. 2. LLE of the system glycerol (1) + ethanol (2) + FAEE (3) at 298 K described by UNIFAC-LLE and UNIFAC-OHgly: (w) mass fraction of the components or pseudocomponent; (○) experimental data; (▬) UNIFAC-LLE (···) UNIFAC-OHgly.

Table 4
Average relative deviations between experimental and calculated mass fractions using UNIFAC-LLE and UNIFAC-OHgly.

	UNIFAC-LLE		UNIFAC-OHgly	
	AD-GRP[a]	AD-ERP[a]	AD-GRP[a]	AD-ERP[a]
Glycerol	0.0534	0.0286	0.0413	0.0090
Ethanol	0.0575	0.1219	0.0093	0.0302
$C_{10}H_{20}O_2$	0.0009	0.0034	0.0049	0.0037
$C_{12}H_{24}O_2$	0.0005	0.0042	0.0026	0.0010
$C_{14}H_{28}O_2$	0.0054	0.0698	0.0203	0.0081
$C_{16}H_{32}O_2$	0.0016	0.0255	0.0035	0.0075
$C_{18}H_{36}O_2$	0.0007	0.0139	0.0008	0.0054
$C_{20}H_{40}O_2$	0.0002	0.0033	0.0001	0.0015
$C_{20}H_{38}O_2$	0.0026	0.0270	0.0004	0.0113
$C_{20}H_{36}O_2$	0.0004	0.0034	0.0001	0.0014

[a] Calculated by: $AD(\%) = \sum_n (|w^{exp} - w^{calc}|)/n$, were n is the number of tie lines.

Another study reported an average deviation and a maximum average deviation of lower than 0.20% and 0.66% (lower than UNIFAC-OHgly), respectively, for systems containing glycerol + methanol or ethanol + several biodiesels using the UNIFAC parameters readjusted through an evolutionary algorithm for minimization of the objective function [43]. On the other hand, another study addressing the readjustment of the UNIFAC parameters for systems containing water + biodiesel reported an average absolute relative deviation of 4.69% [44].

The average molar masses of FAEE per tie line in the GRP and ERP ranged from 221.44 to 236.84 g·mol^{-1} and 245.21 to 246.37 g·mol^{-1}, respectively, as shown in Table 5. The FAEE in the ERP has an average molar mass extremely similar to the FAEE in the overall compositions (246.66 g·mol^{-1}), whereas the GRP shows a decrease of up to 10.23%, indicating a different partition between esters as a result of the carbon chain length. Deviations for these components in the GRP showed an inverse correlation with the ethanol mass fractions in the overall composition. This behavior could result in minor changes in the biodiesel composition during the glycerol-settling step when esters showing a very different molecular size are present.

Three other researches studied the partition of individual ethyl esters in systems containing complex mixtures of ester from natural vegetable oils + glycerol + ethanol, and none reported deviations between the average molar masses of ester mixtures in ERP and in the

Table 5
Individual ester mass fraction in the ERP and GRP.

TL[a]	$C_{10}H_{20}O_2$	$C_{12}H_{24}O_2$	$C_{14}H_{28}O_2$	$C_{16}H_{32}O_2$	$C_{18}H_{36}O_2$	$C_{20}H_{40}O_2$	$C_{20}H_{38}O_2$	$C_{20}H_{36}O_2$	aMM[b] ($g{\cdot}mol^{-1}$)
Ester Rich Phase									
1	0.0198	0.0190	0.2832	0.0983	0.0527	0.0125	0.0936	0.0115	246.37
2	0.0230	0.0222	0.3300	0.1145	0.0611	0.0141	0.1076	0.0132	246.20
3	0.0258	0.0250	0.3686	0.1268	0.0670	0.0157	0.1175	0.0145	245.90
4	0.0275	0.0263	0.3845	0.1315	0.0692	0.0160	0.1211	0.0150	245.65
5	0.0308	0.0287	0.4137	0.1408	0.0738	0.0170	0.1292	0.0159	245.35
6	0.0316	0.0301	0.4358	0.1479	0.0770	0.0175	0.1333	0.0165	245.21
Glycerol Rich Phase									
1	0.0060	0.0044	0.0515	0.0139	0.0059	0.0011	0.0098	0.0014	236.84
2	0.0039	0.0026	0.0263	0.0064	0.0024	0.0004	0.0039	0.0006	232.49
3	0.0022	0.0013	0.0116	0.0024	0.0008	0.0001	0.0013	0.0002	227.55
4	0.0015	0.0008	0.0065	0.0013	0.0004	0.0001	0.0006	0.0001	225.22
5	0.0008	0.0004	0.0024	0.0005	0.0001	0.0001	0.0005	0.0001	225.27
6	0.0004	0.0001	0.0008	0.0002	0.0001	0.0000	0.0002	0.0000	221.44

[a] Tie line identification number.
[b] Average molar mass.

overall compositions of higher than 5.2% [21–23]. These low deviations are probably due to the molecular structure (carbon chain length and number of saturations) of the esters in those systems, which differ from the very heterogeneous molecular structure of ethyl esters from coconut oil.

As observed in Fig. 3, the partition coefficient of all individual ethyl esters increased exponentially with the ethanol mass fraction in the overall composition. This behavior is the result of the higher miscibility of these compounds in GRP caused by the increased ethanol content. The affinity of saturated ethyl ester for the GRP increases as a function of the decrease in the carbon number of the molecules, resulting in partition coefficients for $C_{20}H_{40}O_2$ and $C_{10}H_{20}O_2$ ranging from $1.0{\cdot}10^{-5}$ to $1.2{\cdot}10^{-2}$ and $8.8{\cdot}10^{-2}$ to $3.0{\cdot}10^{-1}$, respectively, for the lowest and highest mass fractions of ethanol in the overall composition. The distribution of ethyl esters $C_{20}H_{40}O_2$, $C_{20}H_{38}O_2$, and $C_{20}H_{36}O_2$, all with the same number of carbon atoms, between the GRP and ERP is correlated with the number of double bonds in the molecule, presenting respective partition coefficients of 0.09, 0.10, and 0.12 for the ethanol mass fraction in the overall composition of 0.39.

Fig. 4 shows the HSPs for each component and for the component mixtures in the GRP and ERP. The contribution of dispersion forces in the ERP is higher than in the GRP as a result of the major content of the ethyl esters. In contrast, the contribution of the molecular permanent dipole–permanent dipole forces and molecular hydrogen bonding are higher in the GRP than in the ERP owing to the higher mass fractions of

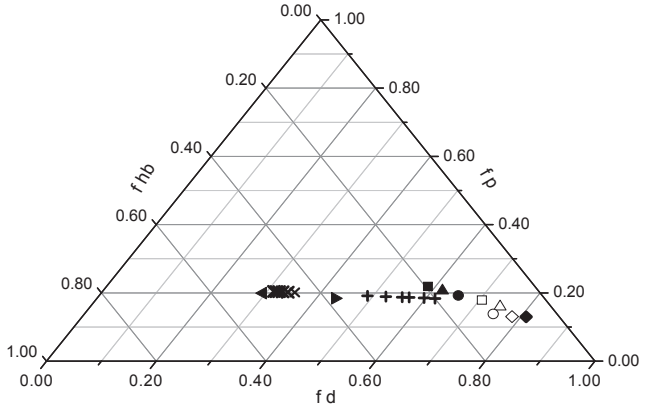

Fig. 4. Hansen Solubility Parameters: (■) $C_{10}H_{20}O_2$; (▲) $C_{12}H_{24}O_2$; (●) $C_{14}H_{28}O_2$; □) $C_{16}H_{32}O_2$; (Δ) $C_{18}H_{36}O_2$; (♦) $C_{20}H_{40}O_2$; (◇) $C_{20}H_{38}O_2$; (○)$C_{20}H_{36}O_2$; (◄)glycerol; (►)ethanol; (×) glycerol-rich phase; (+) ester-rich phase.

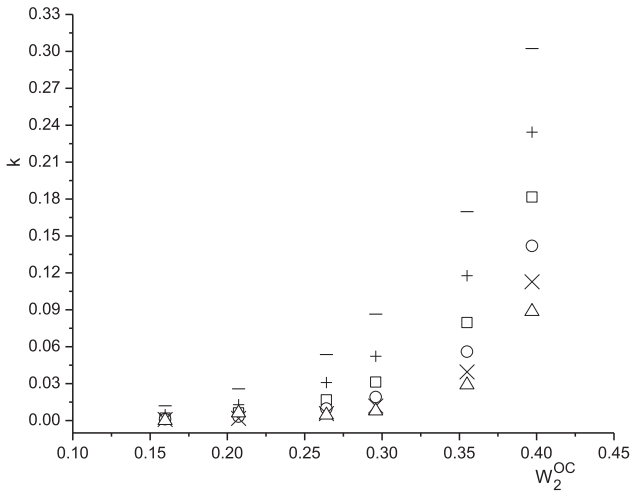

(-)$C_{10}H_{20}O_2$; (+)$C_{12}H_{24}O_2$; (□)$C_{14}H_{28}O_2$; (○)$C_{16}H_{32}O_2$; (×)$C_{18}H_{36}O_2$; (Δ) $C_{20}H_{40}O_2$

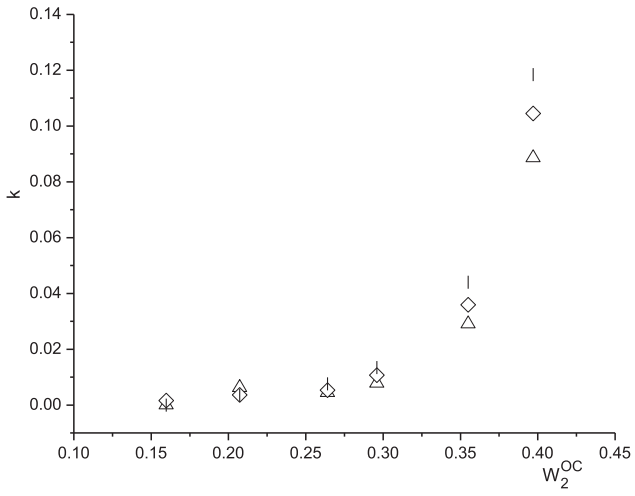

(Δ) $C_{20}H_{40}O_2$; (◊) $C_{20}H_{38}O_2$; (|) $C_{20}H_{36}O_2$

Fig. 3. Distribution coefficients of individual ethyl esters between the glycerol-rich and ester-rich phases as function of ethanol in the overall composition: k distribution coefficient; w_2^{OC} ethanol in the overall composition.

Table 6
Hansen solubility parameters for ethyl esters and for component mixtures in GRP and ERP.

Individual ethyl esters					TL[a]	Component mixture in GRP				Component mixture in ERP			
	δ_d	δ_p	δ_{hb}	δ_t		δ_d	δ_p	δ_{hb}	δ	δ_d	δ_p	δ_{hb}	δ
C10H20O2	15.88	5.93	5.27	17.75	1	16.28	9.30	20.64	27.88	17.40	6.81	11.34	21.86
C12H24O2	15.90	5.31	4.50	17.36	2	15.81	9.44	21.43	28.26	17.41	6.29	9.52	20.82
C14H28O2	15.93	4.68	3.72	17.02	3	15.33	9.46	21.82	28.30	17.39	5.87	8.08	20.06
C16H32O2	15.96	4.05	2.95	16.73	4	14.87	9.39	21.88	28.07	17.39	5.71	7.51	19.78
C18H36O2	15.99	3.42	2.17	16.50	5	14.52	9.33	21.91	27.89	17.33	5.38	6.37	19.23
C20H40O2	16.02	2.79	1.39	16.32	6	14.14	9.25	21.88	27.64	17.31	5.15	5.61	18.91
C20H38O2	16.22	2.92	2.04	16.61									
C20H36O2	16.41	3.04	2.70	16.91									

[a] Tie line identification number.

ethanol and glycerol. These two polar molecules interact, forming permanent dipole–permanent dipole forces, and in a less intense way, hydrogen bonds.

The parameter δ_d is the main association parameter in ethyl esters, and its value increases as a function of the number of carbon atoms because the induced dipole–induced dipole forces are correlated with the surface area of the molecules. In this class of components, the parameters δ_p and δ_H decrease owing to the increase in molecular size, and increase with the unsaturation level in the molecules. This tendency was also observed for δ_p calculated by other authors for methyl esters using the group contribution method presented by Steffanis [45,31]. Experimental determination of the methyl ester dielectric constant, which provides a quantitation of the molecule polarization, confirms this behavior [46]. Because only the COO^- functional groups are responsible for permanent dipole–permanent dipole forces and for hydrogen bonding in the alkyl esters, longer carbon chains hinder the molecular association, reducing δ_p and δ_H.

The previous explanation correlates the mechanism causing the difference in individual ethyl ester partition between the ERP and GRP to the molecular structure and molecular interactions forces using the Hansen solubility parameters. This correlation has the potential to predict and describe the partitioning of other components in several works on liquid–liquid equilibrium, correlating the equilibrium behavior with the physical parameter.

Table 6 shows a reduced difference among δ_t from shorter-chain ethyl esters to the mixture of components in the GRP, as compared to δ_t of longer-chain esters. This tendency is observed in Fig. 4 where the HSPs of larger alkyl esters are more distant from the parameters of the GRP than the HSPs of smaller esters, indicating a greater association of the latter for the GRP. Therefore, this behavior results in lower partition coefficients for longer chain esters reducing the average molar masses of the FAEE in the GRP, causing a diminishing of up to 10.23% with this parameter.

5. Conclusions

The description of the LLE behavior for the system glycerol + ethanol + FAEE from coconut oil at 298 K using the NRTL, UNIFAC-OHgly, and UNIFAC-LLE models resulted in low deviations for the first and second models, and a high deviation for the third. Despite the consideration of pseudocomponents for FAEE, this approach works well for NRTL modeling. The differences in molar mass of ester mixtures in both phases, as compared to FAEE in the overall composition, reached higher than 10% depending on the ethanol content in the overall composition. The experimental data show an increase in the partition of individual ethyl esters to the GRP as a function of the decrease in the molecular size of this class of components. The HSPs correlate this behavior with the reduced difference between δ_p and δ_h for short chain esters as compared to longer chain ethyl esters in relation to the values of these parameters for the mixture of components in the GRP. The HSP approach has the potential to explain the affinity among the many components in this type of system, allowing for an estimate of their distribution during in the equilibrium phases.

Acknowledgments

The authors thank the following funding agencies: Fundação de Amparo à Pesquisa do Estado de Minas Gerais (FAPEMIG) for its financial support (Process: TEC-APQ-01412-16) and for the master's degree scholarship of Vanessa Vilela Lemos; the Conselho Nacional de Desenvolvimento Científico e Tecnológio (CNPq) for its financial support (Process: 420355/2016-2 and Process: 308924/2017-7); the Coordenação de Aperfeiçoamento de Pessoal de Nível Superior – Brasil (CAPES) for its financial support (Finance Code 001); the Fundação de Amparo a Pesquisa do Estado de São Paulo (Process: 08/56258-8) for its financial support; and the Partnerships Program for Education and Training (PAEC, Process: 001/2016) between the Organization of American States (OEA) and the Coimbra Group of Brazilian Universities (GCUB) for the master's degree scholarship of Otto Alberto Quispe Jimenez.

References

[1] Knothe G, Van Gerpen J, Krahl J. The Biodiesel Handbook. 2nd ed. Champaign, Illimois: USA. AOCS Press; 2010.
[2] Peters RA. Fatty alcohol production and use. Inform 1999;7:502–5.
[3] Willing A. Oleochemical esters-environmentally compatible raw materials for oils and lubricants from renewable resources. Fett/Lipid 1999;101:192–8. https://doi.org/10.1002/(SICI)1521-4133(199906)101:6<192::AID-LIPI192>3.0.CO;2-W.
[4] Wehlmann J. Use of esterified rapeseed oil as plasticizer in plastics processing. Fett/Lipid 1999;101:249–2561. https://doi.org/10.1002/(SICI)1521-4133(199907)101:7<249::AID-LIPI249>3.0.CO;2-I.
[5] Bay K, Wanko H, Ulrich J. Biodiesel: high-boiling absorbent for gas purification (Biodiesel: hoch siedendes absorbens fur die gasreinigung). Chem Ing Tech 2004;76:328–33.
[6] Hassan MH, Kalam MA. An overview of biofuel as a renewable energy source: development and challenges. Proc Eng 2013;56:39–53. https://doi.org/10.1016/j.proeng.2013.03.087.
[7] Atabani AE, Silitonga AS, Badruddin IA, Mahlia TMI, Masjuki HH, Mekhilef SA. comprehensive review on biodiesel as an alternative energy resource and its characteristics. Renewable Sustainable Energy Rev 2012;16:2070–93. https://doi.org/10.1016/j.rser.2012.01.003.
[8] Anuar MR, Abdullah AZ. Challenges in biodiesel industry with regards to feedstock, environmental, social and sustainability issues: a critical review. Renewable Sustainable Energy Rev 2016;58:208–23. https://doi.org/10.1016/j.rser.2015.12.296.
[9] Pisarello ML, Dalla-Costa B, Mendow G, Querin CA. Esterification with ethanol to produced biodiesel from high acidity raw materials: Kinetic studies and analysis of secondary reactions. Fuel Process Technol 2010;91:1005–14. https://doi.org/10.1016/j.fuproc.2010.03.001.
[10] Verma P, Sharma MP. Comparative analysis of effect of methanol and ethanol on Karanja biodiesel production and its optimization. 2016;180:164–174, . doi:10.1016/j.fuel.2016.04.035.
[11] Akoh CC, Chang SW, Lee GC, Shaw JF. Enzymatic approach to biodiesel production. J Agric Food Chem 2007;55(22):8995–9005. https://doi.org/10.1021/jf071724y.
[12] Zhang Y, Dubé MA, McLean DD, Kates M. Biodiesel production from waste cooking oil: 1. process design and technological assessment. Bioresour Technol 2003;89(1):1–16. https://doi.org/10.1016/S0960-8524(03)00040-3.
[13] Sawangkeaw R, Teeravitud K, Bunyakiat S, Ngamprasertsith S. Biofuel production

from palm oil with supercritical alcohols: effects of the alcohol to oil molar ratios on the biofuel chemical composition and properties. Bioresour Technol 2011;102(22):10704–10. https://doi.org/10.1016/j.biortech.2011.08.105.
[14] Kariznovi M, Nourozie H, Abedi J. Bitumen characterization and pseudocomponents determination for equation of state modeling. Energy Fuels 2010;24:624–33. https://doi.org/10.1021/ef900886e.
[15] Bogdanic G, Fredeslund A. Prediction of vapor-liquid equilibria for mixtures with copolymers. Ind Eng Chem Res 1995;34:324–31. https://doi.org/10.1021/ie00040a035.
[16] van Grieken R, Coto B, Romero E, Espada JJ. Prediction of liquid-liquid equilibrium in the system furfural + heavy neutral distillate lubricanting oil. Ind Eng Chem Res 2005;44:8106–12. https://doi.org/10.1021/ie050069l.
[17] Buchowski H. Relation between partition coefficients and properties of solvents. Nature 1962;194:674–5.
[18] Hansen CM. The three dimensional solubility parameter – key to paint component affinities: I. solvents plasticizers, polymers and resin. J Paint Technol 1967;39:104–17.
[19] Hansen CM. The three dimensional solubility parameter – key to paint component affinities: III – Independent calculations of parameter components. J Paint Technol 1967;39:511–4.
[20] Hansen CM. Hansen Solubility Parameters: A User's Handbook. 2nd ed. Taylor Francis Group, Boca Raton, FL: CRC Press; 2007.
[21] Basso RC, Meirelles AJA, Batista EAC. Liquid-liquid equilibrium of pseudoternary systems containing glycerol + ethanol + ethylic biodiesel from crambe oil (Crambe abyssinica) at T/K = (298.2, 318.2, 338.2) and thermodynamic modeling. Fluid Phase Equilib 2012;333:55–62. https://doi.org/10.1016/j.fluid.2012.07.018.
[22] Basso RC, Silva CAS, Sousa CO, Meirelles AJA, Batista EAC. LLE experimental data, thermodynamic modeling and sensitivity analysis in the ethyl biodiesel from macauba pulp oil settling step. Bioresour Technol 2013;131:468–75. https://doi.org/10.1016/j.biortech.2012.12.190.
[23] Basso RC, Meirelles AJA, Batista EAC. Experimental data, thermodynamic modeling and sensitivity analyses for the purification steps of ethyl biodiesel from fodder radish oil production. Braz J Chem Eng 2017;34:341–53. https://doi.org/10.1590/0104-6632.20170341s20140197.
[24] Bessa LCBA, Ferreira MC, Abreu CRA, Batista EAC, Meirelles AJA. A new UNIFAC parameterization for the prediction of liquid-liquid equilibrium of biodiesel systems. Fluid Phase Equilib 2016;425:98–107. https://doi.org/10.1016/j.fluid.2016.05.020.
[25] Marcilla A, Ruiz F, Garcia AN. Liquid-liquid-solid equilibria of the quaternary system water – ethanol – acetone – sodium chloride at 25 °C. Fluid Phase Equilib 1995;112:273–89. https://doi.org/10.1016/0378-3812(95)02804-N.
[26] Rodrigues CEC, Silva FA, Marsaioli Jr A. Deacidification of Brazil nut and Macadamia nuts oil by solvent extraction: liquid-liquid data at 298.2 K. J Chem Eng Data 2005;50:517–23. https://doi.org/10.1021/je049687j.
[27] Stragevitch L, d'Ávila SG. Application of a generalized maximum likelihood method in the reduction of multicomponent liquid-liquid equilibrium data. Braz J Chem Eng 1997;14:41–52. https://doi.org/10.1590/S0104-66321997000100004.
[28] Fredenslund A, Jones RL, Prausnitz JM. Group-contribution estimation of activity coefficients in nonideal liquid mixtures. AIChE J 1975;21:1086–99. https://doi.org/10.1002/aic.690210607.
[29] Magnussen T, Rasmussen P, Fredenslund A. UNIFAC parameter table for prediction of liquid-liquid equilibrium. Ind Eng Chem Process Des Dev 1981;20:331–9. https://doi.org/10.1021/i200013a024.
[30] Stefanis E, Panayiotou C. Prediction of Hansen solubility parameters with new group-contribution method. Int J Thermophys 2008;29:568–85. https://doi.org/10.1007/s10765-008-0415-z.
[31] Stefanis E, Panayiotou C. A new expanded solubility parameter approach. Int J Pharm 2012;426:29–43. https://doi.org/10.1016/j.ijpharm.2012.01.001.
[32] Constantinou L, Gani R, O'Connel JP. Estimation of the acentric fator and liquid molar volume at 298 Kusing a new group contribution method. Fluid Phase Equilib 1995;103:11–22. https://doi.org/10.1016/0378-3812(94)02593-P.
[33] Teas JP. Graphic analysis of resin solubilities. J Paint Technol 1968;40:19–25.
[34] Gervagio GC. Fatty acid and derivatives from coconut oil 1–56 In: Foreidoon S, editor. Bailey's Industrial Oils and Fatty Products: Industrial and Nonedible Products from Oils and Fats6th ed.Wiley-Interscience; 2005.
[35] Nakpong P, Wootthikanokkhan S. High free fatty acid coconut oil as a potential feedstock for biodiesel production in Thailand. Renewable Energy 2010;35:1682–7. https://doi.org/10.1016/j.renene.2009.12.004.
[36] Biermann U, Bornscheuer U, Meier MAR, Metzger JO, Schafer HJ. Raw materials: oils and fats as renewable raw materials in chemistry. Andwandte Chemie International Edition 2011;50:3854–71. https://doi.org/10.1002/anie.201002767.
[37] Andreatta AE, Casás LM, Hegel P, Bottini SB, Brignole EA. Phase equilibria in ternary mixtures of methyl oleate, glycerol, and methanol. Ind Eng Chem Res 2008;47:5157–64. https://doi.org/10.1021/ie0712885.
[38] Csernica SN, Hsu JT. Reverse-phase ternary phase diagram, tie lines, and plait point for commercial biodiesel-glycerol-methanol. Ind Eng Chem Res 2011;50:1012–6. https://doi.org/10.1021/ie101262u.
[39] Roostami M, Raeissi S, Mahmoudi M, Nowtoozi M. Liquid-liquid phase equilibria of systems of palm and soya biodiesels: experimental and modeling. Ind Eng Chem Res 2012;51:8302–7. https://doi.org/10.1021/ie300093p.
[40] Esipovich AL, Rogozhin AE, Belousov AS, Kanakov EA, Otopkova KV, Danov SM. Liquid-liquid equilibrium in the systems FAMEs + vegetable oil + methyl alcohol and FAMEs + glycerol + methyl alcohol. Fuel 2018;217:31–7. https://doi.org/10.1016/j.fuel.2017.12.083.
[41] Gonçalves JD, Aznar M, Santos GR. Liquid-liquid equilibrium systems containing Brazil nut biodiesel + methanol + glycerin at 303.15 K and 323.15 K. Fuel 2014;133:292–8. https://doi.org/10.1016/j.fuel.2014.05.004.
[42] Basso RC, Miyake FH, Meirelles AJA, Batista EAC. Liquid-liquid equilibrium data and thermodynamic modeling at T/K = 298.2, in the washing step of ethyl biodiesel production from crambe, fodder radish and macauba pulp oils. Fuel 2014;117:590–7. https://doi.org/10.1016/j.fuel.2013.09.020.
[43] Noriega MA, Narváez PC, Imbachi AD, Cadavid JG, Habert AC. Liquid-liquid equilibrium for biodiesel-glycerol-methanol or ethanol systems using UNIFAC correlated parameters. Energy 2016;111:841–9. https://doi.org/10.1016/j.energy.2016.06.031.
[44] Roosta A. New group interaction parameters of the UNIFAC model for the solubility of water in fatty acid methyl esters and biodiesel. Fuel 2018;220:339–44. https://doi.org/10.1016/j.fuel.2018.02.024.
[45] Batista MM, Guirardello R, Krahenbul MA. Determination of the solubility parameters of biodiesel from vegetable oils. Energy Fuels 2013;27:7497–509. https://doi.org/10.1021/ef401690f.
[46] Gouw TH, Vlugter JC. Physical properties of fatty acid methyl esters V. dielectric constant. J Am Oil Chem Soc 1964;41:675–8. https://doi.org/10.1007/BF02661406.